Title
Results from Super-Kamiokande and K2K

Journal
Pramana, 60(2)

ISSN
0304-4289

Authors
Vagins, M. R
Super-Kamiokande Collaboration, .
K2K Collaboration, .

Publication Date
2003-02-01

DOI
10.1007/BF02706408

PRAMANA
— journal of
physics

Vol. 60, No. 2
February 2003
pp. 249–259

Results from Super-Kamiokande and K2K

M R VAGINS for the Super-Kamiokande and K2K Collaborations
Department of Physics and Astronomy, University of California, Irvine, 4129 Reines Hall, CA 92697, USA

Abstract. Results from Super-Kamiokande-I's entire 1496 live days of solar neutrino data are presented, including the absolute flux, energy spectrum, zenith angle (day/night) and seasonal variation. The possibility of MSW and vacuum oscillations is discussed in light of these results. Results from the first 1289 days of Super-K-I's atmospheric neutrino analysis are also presented, including the evidence for $\nu_\mu \to \nu_\tau$ oscillations, against $\nu_\mu \to \nu_{\text{sterile}}$ oscillations, and the current limits on proton decay. Finally, results based on 5.6×10^{19} protons on target are given for the K2K long-baseline neutrino oscillation experiment.

Keywords. Neutrino; solar; atmospheric; oscillation; long-baseline.

PACS Nos 14.60.Lm; 14.60.Pq; 14.20.Dh; 11.30.Fs; 26.65.+t

1. Introduction

Super-Kamiokande is the product of the collaborative effort of approximately 110 Japanese and American astrophysicists, many of whom previously worked on either the Kamiokande or IMB water Cherenkov experiments. The Super-Kamiokande site is about 300 km west–northwest of Tokyo near the small town of Mozumi in the Japanese Alps. Located under 1 km of rock (2700 m water equivalent) in the same ancient zinc mine as the old Kamiokande detector and the new KamLAND experiment, Super-K shares the same basic design as its former neighbor and namesake: a cylinder of ultra-pure water surrounded with inward-facing photomultiplier tubes (PMT's), a light barrier, a layer of outward-facing PMT's, and a veto region of water, all contained within a stainless steel tank.

Roughly an order of magnitude larger than its predecessors, Super-K has been designed to be a premier facility for studying solar neutrinos, atmospheric neutrinos, nucleon decay, and neutrinos from galactic supernovae. Weighing in at 50,000 tons of water, and holding over 11,000 inward-facing fifty-centimeter diameter PMT's and 1850 outward-facing twenty-centimeter PMT's, Super-K is the world's largest underground water Cherenkov detector. Figure 1 shows a cutaway view of the detector.

Beginning in late spring of 1999, a new experiment, KEK to Kamioka (K2K), started taking data. As seen in figure 2, this project directs a beam of artificially produced muon neutrinos through Japan from the KEK accelerator laboratory outside Tokyo all the way through central Japan to Super-K, some 250 km distant. A one kton water Cherenkov detector, essentially a 2% scale model of Super-K located 300 m from the end of the neutrino

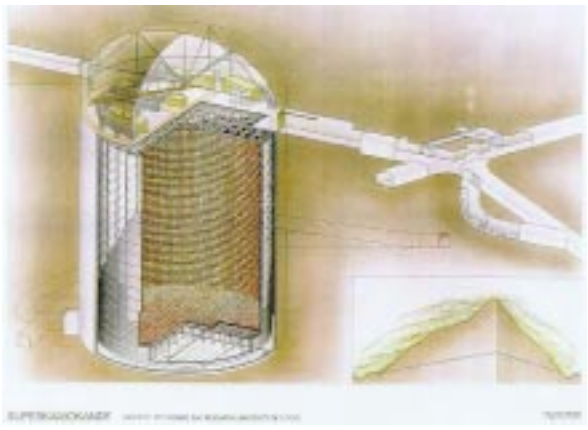

Figure 1. Cutaway view of the Super-Kamiokande detector. The detector itself stands some 42 m tall – to get a sense of the scale, consider that the tunnels shown in the drawing are large enough for full-sized trucks to drive through. The curving tunnel on the right side of the sketch contains our water purification plant; just above that is our main control room.

Figure 2. The KEK to Kamioka (K2K) experiment.

production region, is used to normalize the neutrino flux. Deviations in the number of events seen in Super-K from the expected number based on simple geometric considerations will serve as additional evidence in support of neutrino oscillations.

On November 12th, 2001, while the detector was being refilled with water after a summer of refurbishment work, a chain reaction of imploding PMT's destroyed 6777 of the inner tubes and about 1100 of the outer tubes. An intensive investigation into the cause(s) and future prevention of such a calamity was immediately begun. As a result of this inquiry, additional pressure housings were designed and tested for the large inner PMT's, and rebuilding began in early 2002. Super-Kamiokande is expected to be back on line with its full complement of outer tubes and about 50% of its difficult-to-manufacture inner tubes (rearranged to provide even coverage) by the end of 2002. Its physics reach, especially at higher energies, will be only modestly affected. Nevertheless, before the new JHF machine turns on and sends an intense long-baseline neutrino beam to Mozumi in 2007, Super-K will be restored to its full inner PMT coverage.

2. Low energy analysis – Solar neutrinos at Super-Kamiokande

2.1 *Solar intro*

When we talk about Super-Kamiokande's 'low-energy' analysis, we generally mean events with less than 100 MeV of visible energy deposited in the detector. With an endpoint energy of about 15.0 MeV, Super-Kamiokande's primary source of solar neutrinos is the following nuclear reaction in the sun:

$$^8\mathrm{B} \rightarrow ^8\mathrm{Be}^* + e^+ + \nu_\mathrm{e}. \tag{1}$$

These ^{8}B neutrinos are seen in Super-K via elastic scattering:

$$\nu_\mathrm{e} + e^- \rightarrow \nu_\mathrm{e} + e^-. \tag{2}$$

We have obtained what is by far the largest single sample of solar neutrino events in the world. Our most recent results, representing 1496 live days of analyzed low-energy data, spanning the period of May 31, 1996 to July 15, 2001, will be presented now.

2.2 *Recent results of the solar neutrino analysis*

Our standard method of displaying the solar neutrino signal is through the use of $\cos\theta_{\mathrm{sun}}$ plots, where $\cos\theta_{\mathrm{sun}}$ is the angle between a reconstructed low-energy event's direction and the direction defined by a line drawn between the sun's current position and the vertex position.

The solar neutrino signal for the energy range 5.0 MeV to 20.0 MeV is shown as the left plot in figure 3. The peak above the background in the direction of $\cos\theta_{\mathrm{sun}} = 1$ (i.e., originating from the direction of the sun) are our solar neutrinos. There are some 22,400 events under the peak and above the background. Note that, unlike atmospheric neutrinos, one can only identify solar neutrinos in a statistical fashion. No one has yet devised a way to prove that any given event in our detector actually originated from the sun. For this reason, reducing the sea of background events under the solar peak is of central importance in all low-energy investigations.

The best fit to the data points is given by the flux predicted by the BP2000 version of the standard solar model [1a] multiplied by a factor of 46.5%. More specifically, we measure

$$\mathrm{Flux} = 2.35 \pm 0.02(\mathrm{stat.}) \pm 0.08(\mathrm{syst.}) \times 10^6/\mathrm{cm}^2/\mathrm{s} \tag{3}$$

and

$$\frac{\mathrm{Data}}{\mathrm{SSM}_{\mathrm{BP2000}}} = 0.465 \pm 0.005(\mathrm{stat.}) \pm 0.016(\mathrm{syst.}) \tag{4}$$

The plot on the left side of figure 3 contains all the low-energy data – if the data are broken down into bins based on where the sun was in relation to the horizon at the time the signal was received we get the right side plot of figure 3. The bins on the right side of the plot are defined within the figure. At present our value for the overall day/night difference is as follows:

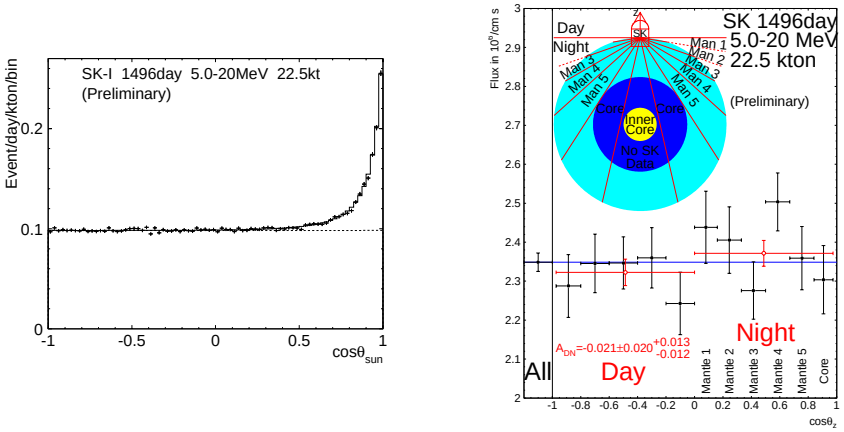

Figure 3. *Left*: Solar neutrino signal between 5.0 MeV and 20.0 MeV. The line is a fit to 46.5% of the BP2000 SSM. *Right*: Variation of the solar neutrino flux as a function of zenith angle. Both plots are the result of 1496 live days of data and a 22.5 kton fiducial volume.

$$\frac{D-N}{(D+N)/2} = -0.021 \pm 0.020(\text{stat.}) \pm 0.013(\text{syst.}) \tag{5}$$

Another interesting study which can be performed by breaking up the data is the search for seasonal variations in the flux. Such variations would be due to vacuum oscillations as the earth moves around the sun. Our results are shown on the left side plot in figure 4. The wavy line represents the expected $1/r^2$ variation in the flux due to eccentricity of the earth's orbit. It can be seen that the fit to the expected no-vacuum-oscillation line is rather good.

Perhaps the most powerful test of oscillations, however, is made by looking at the energy spectrum of the recoil electrons from the ^{8}B solar neutrinos. Assuming that neutrinos are massive, neutrinos of a given energy will have an opportunity to execute a given number (or fractional number) of oscillations before reaching Super-Kamiokande. Therefore, deviations from the predicted spectral shape would constitute rather strong evidence of oscillations, since neutrinos of certain energies would then be more (or less) likely to be seen in our detector than neutrinos of other energies.

The results of our energy spectrum analysis can be seen in the plot on the right side of figure 4, where the data points have been divided by the non-oscillating SSM prediction for each bin. If these points fell in a straight, flat line then they would be consistent with an unoscillated spectrum. In fact, the present shape seen in figure 4 has a very good fit to flat. This lack of deviations will allow us to rule out certain oscillation hypotheses in the next section.

2.3 *Solar neutrino oscillation analysis*

The probability of flavor oscillation (in the simplest, two-component case) is given by the well-known expression

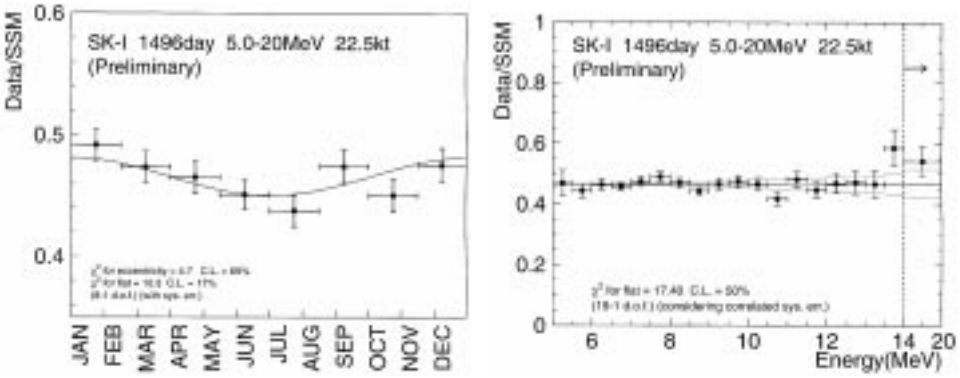

Figure 4. *Left*: Seasonal variation in solar neutrino signal between 5.0 MeV and 20.0 MeV. The wavy line represents the expected $1/r^2$ variation in the flux due to the eccentricity of earth's orbit around the sun. *Right*: Energy spectrum of solar neutrino recoil electrons, divided by theoretical predictions.

$$P(\nu_a \to \nu_b) = \sin^2 2\Theta \sin^2 (1.27\Delta m^2\ [\mathrm{eV}^2] L\ [\mathrm{km}]/E\ [\mathrm{GeV}]). \tag{6}$$

Because of the Δm^2 term, proof of oscillations would provide evidence of at least one non-zero neutrino mass. Indeed, these two phenomena, oscillations and massive neutrinos, are inextricably linked.

By combining SNO's charged-current flux with the fluxes measured by solar neutrino experiments using chlorine and gallium as their detection media, we arrive at the allowed regions in $\tan^2\Theta$ and Δm^2 phase space for oscillations into active neutrino species. The left plot of figure 5 shows the large and small angle MSW solutions, as well as the so-called 'low' region and, at much lower Δm^2, the vacuum (or 'just-so') oscillation solution.

By adding Super-Kamiokande's measured flux and zenith angle spectral information (essentially, how the energy spectrum varies with zenith angle) to this global fit we are left with the right side plot of figure 5. To provide the most general possible result, the ^{8}B and *hep* fluxes are free parameters and are not constrained to any particular solar model. At the 95% confidence level, only the LMA solution survives. Although not shown, oscillations into purely sterile neutrinos are completely ruled out by Super-K's data at the 95% level everywhere in phase space.

3. High energy analysis – Atmospheric neutrinos at Super-Kamiokande

3.1 *Atmospheric intro*

When we talk about Super-Kamiokande's 'high-energy' analysis, we generally mean events with greater than 100 MeV of visible energy deposited in the detector. Our primary source of these events (since proton decay has proven quite elusive!) are the result of interactions of cosmic ray particles with the upper atmosphere.

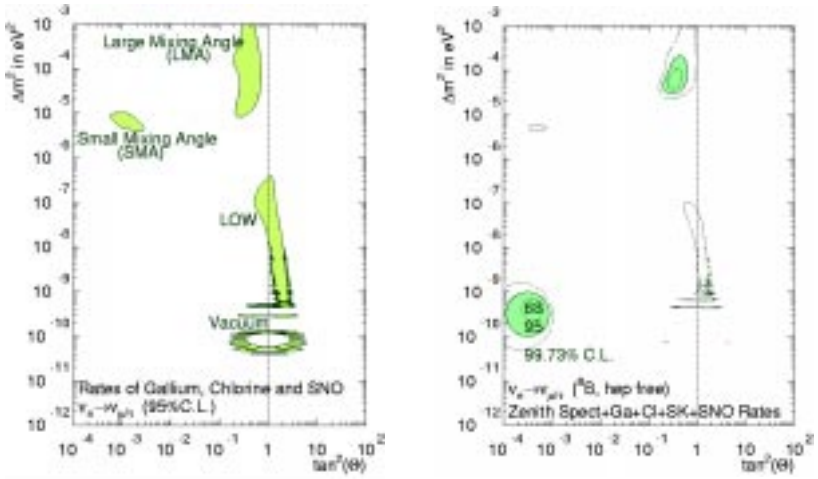

Figure 5. *Left*: The allowed regions in ($\tan^2\Theta$, Δm^2) phase space remaining after the solar neutrino fluxes measured in three types of detectors are combined in a global fit. *Right*: The remaining phase space for oscillations after Super-K's flux and zenith angle information are added. The concentric circular regions at the lower left of this plot are a key to the contours and shading. Shaded areas in both plots are allowed at the 95% confidence level for oscillations into active neutrino species.

Neutrinos of all energies (above about 1 GeV, the flux is well-described by an $E^{2.7}$ power law) are produced in the atmosphere by cosmic ray showers and the cascades

$$\pi/K \to \mu \to e. \tag{7}$$

Each muon produced is associated with a ν_μ and each muon which decays produces a ν_e in addition to a second ν_μ.

Neutrinos arrive at the detector from all directions, with the upward and downward fluxes equal to within about $\pm 10\%$. Neutrinos arriving from above have traveled only about 15 km from their point of production in the atmosphere, while those arriving from below have traversed a distance comparable to the earth's diameter (13,000 km). Thus the atmospheric neutrino flux, spanning many decades of both E and L, provides an ideal beam for studying L/E-dependent oscillation effects.

We have obtained the world's largest sample of atmospheric neutrino events. Our results, representing 1289 live days of analyzed high-energy data, will be presented here.

3.2 *The evidence for oscillations*

For largely historical reasons, our atmospheric data are split into a 'sub-GeV' sample and a 'multi-GeV' sample. The data are further broken up by the number of Cherenkov rings visible in Super-K, and into fully contained (FC) events (no light in the anticounter) and higher-energy, partially contained (PC) events (some light in the anticounter, but not through-going).

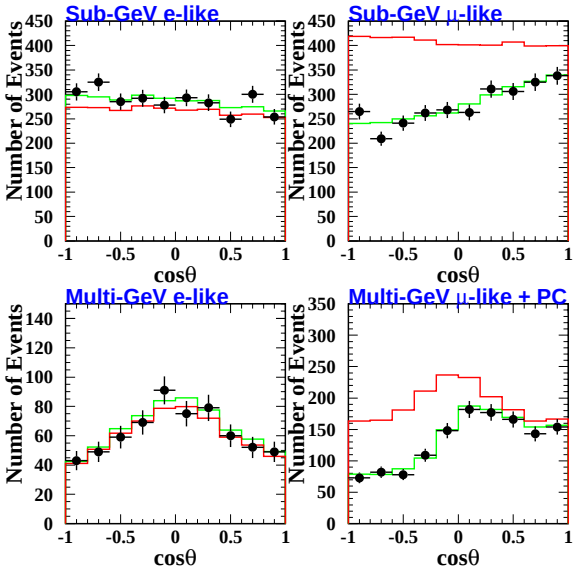

Figure 6. Zenith-angle distributions for 1289 days of atmospheric neutrino data. The upper lines in the μ-like plots are what is expected for no oscillations, and the fit to the data is for the oscillation solution $(\sin^2 2\Theta, \Delta m^2) = (1.00, 2.5 \times 10^{-3}\ \mathrm{eV}^2)$. These four plots are filled with events caused by interactions between atmospheric electron and muon neutrinos with the water in Super-K.

In figure 6 we see plots of the zenith-angle dependence of various high-energy data sets. Here, $\cos\theta = 1.0$ indicates the events which are coming from directly overhead, $\cos\theta = 0.0$ are those events coming from the horizon, and those with $\cos\theta = -1.0$ come from directly underfoot. The top two plots contain sub-GeV events, and the lower two are filled with multi-GeV data. Those two on the left are due to ν_e interactions in Super-K, and the two on the right come from ν_μ interactions. The upper line in the ν_μ plots are the theoretical predictions if there are no oscillations, while the lower line, which passes through almost every data point, is the shape one would expect for $(\sin^2 2\Theta, \Delta m^2) = (1.00, 2.5 \times 10^{-3}\ \mathrm{eV}^2)$. Note that the ν_e-generated events show no angular deviations from the expected (no oscillation) case, while the ν_μ-generated events start to drop off the further from straight down they become. The muon neutrinos seem to know how long they have traveled before being caught by Super-K! This is our smoking gun. What is more, because the e-like events show no excess, we can tell that the oscillations we are seeing are *not* $\nu_\mu \to \nu_e$, but rather must be either $\nu_\mu \to \nu_\tau$ or $\nu_\mu \to \nu_{\mathrm{sterile}}$.

The left side of figure 7 shows the allowed $(\sin^2 2\Theta, \Delta m^2)$ phase space when the data from figure 6 and additional information from upward-going muons (produced by very high-energy neutrinos interacting in the rock below the detector) are combined. The χ^2_{min} for oscillations is 142.1/152 degrees of freedom, while χ^2_{min} for *no* oscillations is 344.1/154 degrees of freedom.

But are we seeing the result of $\nu_\mu \to \nu_\tau$ or $\nu_\mu \to \nu_s$? The right side of figure 7 shows the allowed regions for three possible oscillation scenarios. Overlaid on them are the regions excluded by our studies of neutral current interactions and possible matter effects on

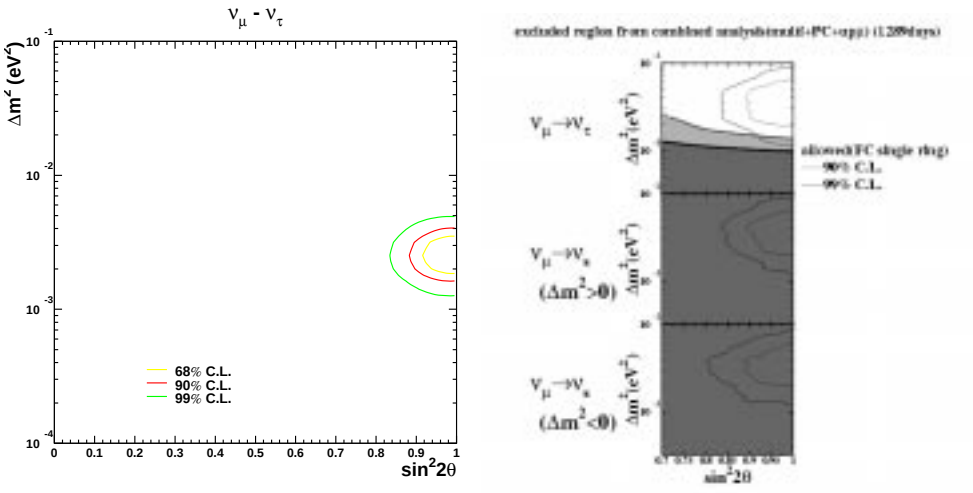

Figure 7. *Left*: Allowed region for atmospheric neutrino oscillations for 1289 days of data. *Right*: The allowed regions for oscillations in three possible oscillation hypotheses overlaid with the excluded regions (shaded areas below the lines are excluded: light gray at 90% and dark gray at 99%) from our $\nu_\mu \to \nu_\tau$ vs. $\nu_\mu \to \nu_s$ analyses. The $\nu_\mu \to \nu_\tau$ allowed region is completely unconstrained, while the entire phase space for both possible $\nu_\mu \to \nu_s$ solutions are excluded at better than the 99% confidence level. We therefore conclude that Super-K is seeing the results of $\nu_\mu \to \nu_\tau$ oscillations.

the oscillation of upward-going high-energy events. The upshot is that while the allowed region for $\nu_\mu \to \nu_\tau$ survives, the entire allowed region for $\nu_\mu \to \nu_s$ is completely excluded at better than 99% regardless of whether or not ν_μ is more massive than ν_s. We therefore conclude that we are indeed seeing the result of $\nu_\mu \to \nu_\tau$ oscillations in Super-Kamiokande and believe $\nu_\mu \to \nu_s$ oscillations to be conclusively ruled out by our data.

3.3 *Nucleon decay*

In many ways, this whole large water Cherenkov business got its start in the early 1980's as a means to search for proton decay. In those days, the leading unified theory, $SU(5)$, predicted that protons would decay at a rate which would be easily observable in such detectors. Of course, it has turned out that protons have a lifetime at least 10,000 times greater than that predicted by minimal $SU(5)$, and some twenty years later we are still looking for our first gold-plated event. Large water detectors are now seen primarily as neutrino observatories, not proton decay experiments – the meaning of the trailing 'NDE' was quietly changed from 'nucleon decay experiment' in Kamiokande to 'neutrino detection experiment' in Super-Kamiokande. Nevertheless, because nucleon decays would produce background events in our atmospheric neutrino sample (a somewhat ironic inversion of what was expected in the past), we can get nucleon decay lifetime limits from our high-energy data at very little additional cost.

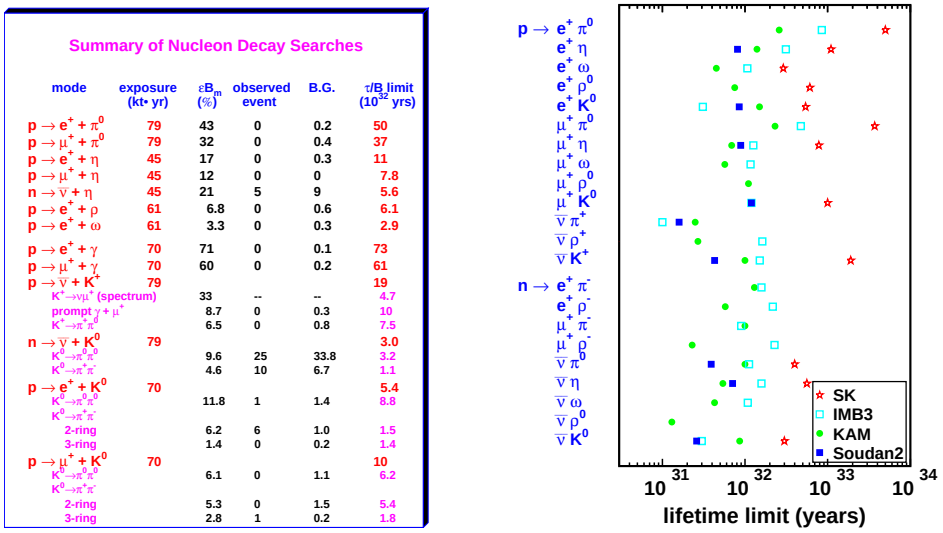

Summary of Nucleon Decay Searches

mode	exposure (kt• yr)	εB_m (%)	observed event	B.G.	τ/B limit (10^{32} yrs)
$p \to e^+ + \pi^0$	79	43	0	0.2	50
$p \to \mu^+ + \pi^0$	79	32	0	0.4	37
$p \to e^+ + \eta$	45	17	0	0.3	11
$p \to \mu^+ + \eta$	45	12	0	0	7.8
$n \to \bar{\nu} + \eta$	45	21	5	9	5.6
$p \to e^+ + \rho$	61	6.8	0	0.6	6.1
$p \to e^+ + \omega$	61	3.3	0	0.3	2.9
$p \to e^+ + \gamma$	70	71	0	0.1	73
$p \to \mu^+ + \gamma$	70	60	0	0.2	61
$p \to \bar{\nu} + K^+$	79				19
$K^+ \to \nu\mu^+$ (spectrum)		33	--	--	4.7
prompt $\gamma + \mu^+$		8.7	0	0.3	10
$K^+ \to \pi^+\pi^0$		6.5	0	0.8	7.5
$n \to \bar{\nu} + K^0$	79				3.0
$K^0 \to \pi^0\pi^0$		9.6	25	33.8	3.2
$K^0 \to \pi^+\pi^-$		4.6	10	6.7	1.1
$p \to e^+ + K^0$	70				5.4
$K^0 \to \pi^0\pi^0$, $K^0 \to \pi^+\pi^-$		11.8	1	1.4	8.8
2-ring		6.2	6	1.0	1.5
3-ring		1.4	0	0.2	1.4
$p \to \mu^+ + K^0$	70				10
$K^0 \to \pi^0\pi^0$, $K^0 \to \pi^+\pi^-$		6.1	0	1.1	6.2
2-ring		5.3	0	1.5	5.4
3-ring		2.8	1	0.2	1.8

Figure 8. *Left*: Nucleon decay limits for 1289 live days (79 kton years) of data. *Right*: Comparison of nucleon decay limits from various detectors.

Figure 8 shows our current lifetime limits for various decay modes. Although there seems to be an excess of events beyond what is predicted for background in a few of the modes involving $K^0 \to \pi^+\pi^-$ decays in the final state, the lack of a corresponding excess in the twice-as-common $K^0 \to \pi^0\pi^0$ final state modes make us think that these are not real nucleon decays but rather the result of some novel background.

4. Long-baseline neutrino oscillation experiment – K2K

K2K had collected about half of its total planned protons-on-target when the accident at Super-Kamiokande temporarily put both projects on hold. Finishing the job started by K2K in 1999 is one of the primary motivations for the rapid reconstruction of Super-K. However, with 5.6×10^{19} protons now delivered, the initial results from K2K are quite encouraging.

After passing a series of cuts almost identical to those used to extract atmospheric neutrino events in Super-Kamiokande, events originating from the accelerator at KEK are identified at Kamioka using GPS-based timing. After the time-of-flight delay is subtracted, these high-energy events at Super-K must occur within about $1.3\,\mu$s of the beam extraction. This timing cut drastically reduces any atmospheric neutrino backgrounds.

Using the well-characterized flux of neutrinos at the near detectors, at this point we would expect to have seen 80 ± 8 events inside Super-Kamiokande's 22.5 kton fiducial volume. We have instead seen just 56 events. Assuming that the neutrinos are not being missed for some other reason (and many timing and beam stability studies assure us they are not) this rate reduction implies that only a 2.3% probability of no oscillations remains. As seen in figure 9, the oscillation phase space regions excluded by K2K neatly bracket

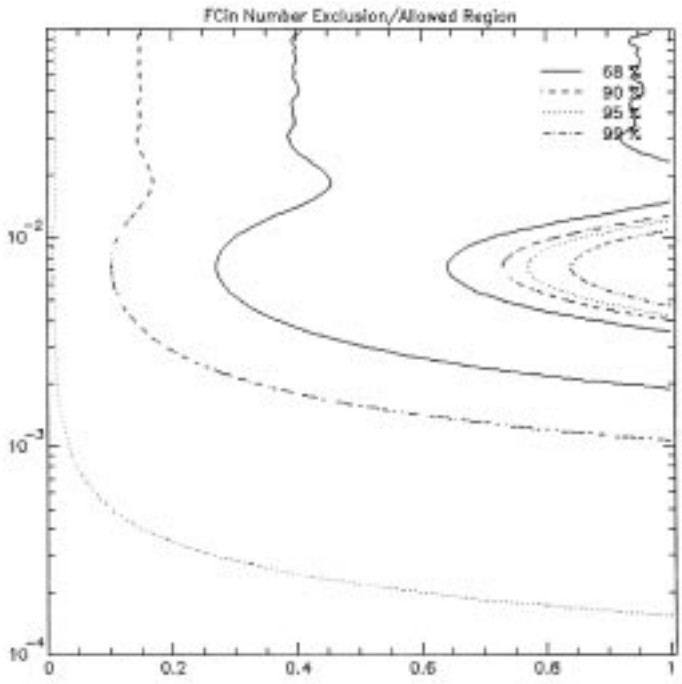

Figure 9. Excluded regions from K2K overlaid on Super-K's allowed region for atmospheric neutrino oscillations. The allowed region is contained within the non-excluded phase space. In this plot the *x*-axis shows $\sin^2 2\Theta$, while the *y*-axis depicts Δm^2 in units of eV^2.

the allowed region from Super-K's atmospheric neutrino analysis. Given these tantalizing results, it is clear why we hope to collect the second half of K2K's data as soon as possible.

References

[1] Measurement of a small atmospheric ν_μ/ν_e ratio, The Super-Kamiokande Collaboration, *Phys. Lett.* **B433**, 9 (1998)

[1a] J Bahcall, S Basu and M Pinsonneault, *Astrophys. J.* **555**, 990 (2001)

[2] Measurements of the solar neutrino flux from Super-Kamiokande's first 300 days, The S-K Collaboration, *Phys. Rev. Lett.* **81**, 1158 (1998)

[3] Evidence for oscillation of atmospheric neutrinos, The S-K Collaboration, *Phys. Rev. Lett.* **81**, 1562 (1998)

[4] Study of the atmospheric neutrino flux in the multi-GeV energy range, The S-K Collaboration, *Phys. Lett.* **B436**, 33 (1998)

[5] Search for proton decay via $p \to e^+\pi^0$ in a large water Cherenkov detector, The S-K Collaboration, *Phys. Rev. Lett.* **81**, 3319 (1998)

[6] Calibration of Super-Kamiokande using an electron LINAC, The S-K Collaboration, *Nucl. Instrum. Methods* **A421**, 113 (1999)

[7] Measurement of radon concentrations at Super-Kamiokande, The S-K Collaboration, *Phys. Lett.* **B452**, 418 (1999)
[8] Neutrino induced upward stopping muons in Super-Kamiokande, The S-K Collaboration, *Phys. Lett.* **B467**, 185 (1999)
[9] Constraints on neutrino oscillation parameters from the measurement of day night solar fluxes at Super-Kamiokande, The S-K Collaboration, *Phys. Rev. Lett.* **82**, 1810 (1999)
[10] Measurement of the solar neutrino energy spectrum using neutrino electron scattering, The S-K Collaboration, *Phys. Rev. Lett.* **82**, 2430 (1999)
[11] Measurement of the flux and zenith angle distribution of upward through going muons, The S-K Collaboration, *Phys. Rev. Lett.* **82**, 2644 (1999)
[12] Observation of an east–west anisotropy of the atmospheric neutrino flux, The S-K Collaboration, *Phys. Rev. Lett.* **82**, 5194 (1999)
[13] Search for proton decay via $p \to \overline{\nu} K^+$ in a large water Cherenkov detector, The S-K Collaboration, *Phys. Rev. Lett.* **83**, 1529 (1999)
[14] Design, construction, and operation of SciFi tracking detector for K2K experiment, The K2K Collaboration, *Nucl. Instrum. Methods* **A453**, 165 (2000)
[15] N-16 as a Calibration Source for Super-Kamiokande, The S-K Collaboration, *Nucl. Instrum. Methods* **A458**, 638 (2000)
[16] Tau neutrinos favored over sterile neutrinos in atmospheric muon-neutrino oscillation, The S-K Collaboration, *Phys. Rev. Lett.* **85**, 3999 (2000)
[17] Detection of accelerator produced neutrinos at a distance of 250-Km, The K2K Collaboration, *Phys. Lett.* **B511**, 178 (2001)
[18] Solar B-8 and hep neutrino measurements from 1258 days of Super-Kamiokande data, The S-K Collaboration, *Phys. Rev. Lett.* **86**, 5651 (2001)
[19] Constraints on neutrino oscillations using 1258 days of Super-Kamiokande solar neutrino data, The S-K Collaboration, *Phys. Rev. Lett.* **86**, 5656 (2001)